A model for amyloid fibril formation in immunoglobulin light chains based on comparison of amyloidogenic and benign proteins and specific antibody binding

Ritu Khurana[1#], Pierre O. Souillac[1], Alisa C. Coats[1], Lauren Minert[1], Cristian Ionescu-Zanetti[2], Sue A. Carter[2], Alan Solomon[3] and Anthony L. Fink[1]

1. Department of Chemistry and Biochemistry, University of California, Santa Cruz, CA 95064 USA
2. Department of Physics, University of California, Santa Cruz, CA 95064 USA
3. Human Immunology and Cancer Program, Department of Medicine, University of Tennessee Graduate School of Medicine, Knoxville, TN USA

\# Present address: Division of Molecular and Structural Biology, Central Drug Research Institute, Lucknow, 226001 India

KEY WORDS: *AL amyloidosis, antibody, amyloid fibrillation, structure, stability, AFM*

ABBREVIATIONS: *CD = circular dichroism; V_L = immunoglobulin light chain variable domain; LEN, SMA = immunoglobulin light chain variable domains from patients with these initials; ATR-FTIR = attenuated total reflectance Fourier transform infrared spectroscopy; ThT = Thioflavin T; AFM = atomic force microscopy*

Abstract

In an attempt to understand the mechanism of amyloid fibril formation in light chain amyloidosis, the properties of amyloidogenic (SMA) and benign (LEN) immunoglobulin light chain variable domains (V_L) were compared. The conformations of LEN and SMA were measured using secondary and tertiary structural probes over the pH range from 2 and 8. At all pH values, LEN was more stable than SMA. The CD spectra of LEN at pH 2 were comparable to those of SMA at pH 7.5, indicating that the low pH conformation of LEN closely resembles that of SMA at physiological pH. At low pH, a relatively unfolded intermediate conformation is populated for SMA and rapidly leads to amyloid fibrils. The lack of such an intermediate with LEN, is attributed to sequence differences and accounts for the lack of LEN fibrils in the absence of agitation. A κIV-specific monoclonal antibody that recognizes the N-terminal of SMA caused unraveling of the fibrils to the protofilaments and was observed to bind to one end of SMA protofilaments by atomic force microscopy. The antibody result indicates that each protofilament is asymmetric with different ends. A model for the formation of fibrils by SMA is proposed.

Amyloidosis involves deposits of normally soluble proteins either neurologically, or systemically. Amyloidogenic proteins sometimes undergo proteolysis before formation of fibrils, as with immunoglobulin light chains and apo-SAA in AL and AA amyloidosis, respectively. In some cases, fibril formation is associated with specific mutations, for example, transthyretin, apo A-1, gelsolin, cystatin C, lysozyme (reviewed in[1,2]).

Immunoglobulin (Ig) light chain deposition diseases involve both fibrils, as in AL (or light chain) amyloidosis, or amorphous aggregates, as in light chain deposition disease (LCDD)[3]. Various sequences of Bence Jones proteins have been characterized and their propensities to aggregate have been studied[4,5]. A detailed analysis of amyloidogenic, amorphous aggregate-forming or non-aggregating light chains revealed a significant decreased stability for the

Correspondence: Dr. Anthony L. Fink, Department of Chemistry and Biochemistry, University of California, Santa Cruz, CA 95064 USA
Tel: 831 459-2744 Fax: 831 459-2744 or 831 459-2935 E-mail: enzyme@cats.ucsc.edu

Submitted: October 7, 2002 Revision Accepted: April 24, 2003

amyloidogenic chains[6]. Recombinant Ig light chains have also been studied and again the amyloidogenic chains were shown to be less stable than the benign ones[7-10]. The variation within the Ig light chain variable domain sequences makes the molecular basis of protein aggregation both interesting and challenging to decode.

Both SMA and LEN (initials of the patients) belong to the κIV family of Ig light chains. SMA was extracted from lymph node-derived amyloid fibrils of an AL amyloidosis patient[11], whereas LEN, was collected from the urine of a patient with multiple myeloma who showed no evidence of renal dysfunction or amyloidosis[12]. The sequences of SMA and LEN are very similar; only eight amino acids differ out of 114. Four of these residues are in CDR3 (Q89H, T94H, Y96Q, S97T), two are in CDR1 (S29N, K30R) and the remaining two in the framework region (P40L, I106L). A detailed study by Raffen *et al*[13] of SMA-like mutations in LEN showed that only the Y96Q, Q89H, and P40L mutations decreased the stability significantly. Other point mutations S29N, T94H, and S97T actually increased the stability of LEN. Analysis of the mutations revealed that the stability difference between LEN and SMA could be accounted for by the sum of the stability differences of the individual point mutations, and that no two mutants acted synergistically to significantly reduce the stability of SMA[13]. The high-resolution crystallographic structure of LEN (1.8 Å) has been solved (PDB Accession No. 1LVE)[14] and is shown in Figure 1, in which the positions of the substitutions in SMA are indicated. Recently, we reported the existence of two partially-folded intermediate conformational states of SMA as the pH is decreased: a relatively native-like intermediate, I_N, observed between pH 4 and 6, and a more unfolded, but compact, intermediate, I_U, below pH 3[15]. The I_U intermediate readily forms amyloid fibrils, whereas I_N preferentially leads to amorphous aggregates. Except at pH 2, where negligible amorphous aggregate is formed, the amorphous aggregates formed significantly more rapidly than the fibrils. Amorphous aggregates of SMA have also been recently reported in the presence of copper[5]. No such corresponding intermediates have been observed for LEN; however, destabilizing conditions will promote LEN fibrillation[16,17].

In this manuscript, we describe a detailed comparison of the spectroscopic properties and aggregation propensities of LEN and SMA, a closely matched pair of benign and amyloidogenic VLs. Our goal is to understand how the sequence differences between LEN and SMA are responsible for the differences in their propensity to fibrillate.

Materials and methods

Expression and purification of recombinant SMA and LEN

The recombinant V_L domains SMA and LEN were purified from JM83 *E. coli* cells transformed with the plasmid pkIVsma004 and pkIVlen004 respectively, generously provided by Dr. Fred Stevens, Argonne National Lab[18]. The overexpressed proteins were purified using the published procedure with minor modifications[18]. Briefly, the proteins were extracted from the periplasm using osmotic shock via treatment with ice-cold TES followed by cold distilled water. The sucrose and water fractions were pooled together and the periplasmic extract dialyzed against 4 changes of 20 volumes of 10 mM Tris pH 8.0 for LEN or 10 mM acetate buffer pH 5.6 for SMA. The SMA extract was loaded onto a fast-flow SP Sepharose column. The column was washed with 10 mM acetate buffer, pH 5.6 and the protein eluted using 10 mM phosphate buffer, pH 8.0. The fractions were assayed by SDS-PAGE and those containing the recombinant protein were pooled, filtered through 0.22 μ filters, and stored in glass vials at 4°C. Typical yields were 7 to 8 mg of purified protein per liter of cells. LEN extract was passed through High Q cartridges (BioRad) followed by dialysis in 10 mM acetate buffer pH 4.0 and loaded onto a Mono S column using a FPLC system (Pharmacia). The column was washed with 10 mM acetate buffer pH 4.0. LEN was eluted using a salt gradient (from 0 to 120 mM sodium chloride over 20 min). The purest fractions were pooled, dialyzed against 10 mM phosphate buffer pH 8.0, concentrated using Centricon (Millipore) with a 10,000 cut off YM3 membrane, and stored at ~3-4 mg/ml concentrations in glass vials at 4°C. Protein concentrations were measured via optical density at 280 nm using the extinction coefficient of $E_{0.1\%} = 1.8$ calculated from the sequence.

Peptides

Peptides corresponding to the following sequences from SMA, residues 1-13 DIVMTQSPDSLAV; 43-52 PPKLLIYWAS; 59-70 PDRFSGSGSGTD; and 94-107 HPQTFGQGTKLELKG were generously provided by Santa Cruz Biotechnology.

Intrinsic tryptophan fluorescence measurements

Fluorescence measurements were made with a FluoroMax-2 fluorescence spectrometer (Jobin Yvon-Spex). Emission spectra were collected between 300 and 420 nm following excitation at 280 nm. Spectra were collected from pH 2 to 8 using 0.5 μM protein samples in 50 mM of the appropriate buffer with 100 mM NaCl. Spectra were collected at 25 and 37°C. The stability of SMA toward urea denaturation was monitored as a function of pH by recording changes in tryptophan fluorescence intensity upon

excitation at 280 nm and emission at 350 nm at 25°C.

Samples of SMA (1 μM monomer) were incubated in 20 mM phosphate buffer (pH 7.4), 100 mM NaCl containing varying amounts of urea (0 to 8M) for 2 h to ensure completion of the unfolding reaction. Data were analyzed by non-linear least-squares fitting to a two-state folding model. The fraction unfolded, F_u, was calculated using the equation $F_u = (y_f - y)/(y_f - y_u)$ where y represents the observed fluorescence at a particular concentration of urea, and y_f and y_u represent the corresponding fluorescence of the folded and unfolded states respectively at that urea concentration. For baseline fitting, a linear least square analysis was performed to determine the values of y_f and y_u as a function of urea concentration. The free energies of unfolding were calculated as a function of urea concentration using the equation $\Delta G = -RT\ln K_{eq}$, where $K_{eq} = f_u/(1-f_u)$. $\Delta G°$ was determined by linear extrapolation to zero urea concentration using the expression $\Delta G° = \Delta G + m[Urea]$.

ANS binding

1,8-anilinonaphthalene sulfonate was obtained from Kodak. A stock solution in water was filtered through a 0.2 μm syringe filter and the concentration was measured using an extinction coefficient of 5000 $M^{-1}cm^{-1}$ at 350 nm. The fluorescence emission spectra of solutions of 10 μM ANS and 0.5 μM protein were collected at 37°C between 420 and 600 nm upon excitation at 380 nm as a function of pH.

Circular dichroism spectra

CD spectra were collected on an AVIV Model 60 DS spectrometer between 260 and 190 nm for the far-UV region and between 320 and 250 nm for the near-UV region, with a step size of 0.5 nm, an averaging time of 5 s and accumulation of 5 repeats. A 1 cm pathlength cylindrical cell and 0.5 mg/mL protein concentration was used for the near- UV CD measurements, and a 0.01 cm pathlength cylindrical cell and 1.7 mg/ml protein concentration was used for the far-UV CD measurements.

pH-dependence

pH-dependent changes in spectroscopic data were fitted using a modified Henderson-Hasselbalch equation for one (eqn. 1) or two (eqn. 2) transitions, in order to determine the midpoints of the transitions:

$$Y_{obs} = \frac{Y_N + Y_{I_U} 10^{pH-pH_{m2}}}{1+10^{pH-pH_{m2}}} \qquad (1)$$

$$Y_{obs} = \frac{Y_N + Y_{I_N} 10^{pH-pHm1} + \frac{Y_{I_U}}{10^{pH-pH_{m2}}}}{1+10^{pH-pH_{m2}} + \frac{1}{10^{pH-pHm2}}} \qquad (2)$$

where Y_{obs} is the observed spectroscopic property, Y_N is the value of the spectroscopic property for the native state, Y_{IN} is the spectroscopic property for the native-like intermediate, and Y_{IU} is the spectroscopic property for the unfolded-like intermediate. pH_{m1} and pH_{m2} are the midpoints of the transitions from the native state to the I_N intermediate and from the I_N to the I_U intermediates, respectively[19].

Thin film ATR-FTIR

Measurements were performed using a SPECAC out-of-compartment ATR accessory and a Nicolet 800SX FTIR bench. A germanium crystal IRE was used for making hydrated thin-films of ~50 to 100 μg protein from both soluble and insoluble protein, as previously described[20-22]. The sample spectra were Fourier transformed using a clean crystal spectrum as background. The water vapor spectrum was collected by reducing the air purge and subtracted from the protein spectra until the resulting spectra were featureless in the region between 1700 and 1800 cm^{-1}. Spectra for SMA and LEN were collected at pH 7.5 (50 mM sodium phosphate, 100 mM NaCl), and at pH 2.0 (20 mM HCl, 100 mM NaCl).

In vitro fibrillation assays

Fibril formation was monitored using a fluorescence assay based on the enhanced fluorescence of the dye thioflavin T (ThT) on binding to amyloid fibrils[23,24]. Amyloid fibrils were grown from purified protein solution (40 μM) at pH 2.0 (20 mM HCl and 100 mM NaCl) in a 1.8 ml flat-bottomed screw-capped glass vial with and without stirring using a Teflon-coated micro-stir bar. Typical fibril growth experiments involved incubating the protein at 37°C and removing aliquots (10 μL) over time for analysis by ThT binding (see below). ThT fluorescence spectra were collected using a SPEX/Jobin-Yvon Fluoromax-2 spectrofluorometer. ThT binding assays were conducted by adding the protein aliquots (10 μL) to 990 ml of a 20 μM pH 7.5 ThT solution (50 mM TRIS, and 100 mm NaCl) in a 1 mL fluorescence cuvette. Fluorescence emission was monitored at 482 nm (5 nm bandpass), with excitation at 450 nm (5 nm bandpass).

Atomic force microscopy

The samples were imaged with an Autoprobe AFM (Park Scientific, Sunnyvale, CA). The tube scanner was a 100 μm Scanmaster (Park Scientific). Non-contact

ultralevers (Park Scientific) were used as cantilevers. The images were taken in air, at a scan frequency of 1-2 Hz. in non-contact AFM (NC-AFM) imaging mode. Samples were prepared for AFM imaging by drying a 5 ml sample from the reaction mixture on freshly cleaved mica with nitrogen gas. The buffer was washed from the surface of the mica with double distilled water and the mica was dried again.

Antibody binding to SMA fibrils

The 11-1F4 antibody was prepared as described[25]. SMA fibrils were made by stirring a 0.5 mg/ml SMA solution at pH 5, 37°C, for 4 days. Then 100 μL of the incubated solution was spun at 14000 rpm in a microfuge. The pellet was washed twice with deionized water to remove the loosely pelleted amorphous material. The resuspended fibrils were incubated with 10 μL of 1 mg/mL solution of 11-1F4 antibody for 30 min after brief treatment in a water bath sonicator. The preparation was centrifuged again, the supernatant (with excess antibody) was removed and the pellet resuspended in 10 μL of deionized water before loading on to freshly cleaved mica.

Determining the specificity of antibody 11-1F4 using peptides derived from SMA

Reacti-bind maleic anhydride activated polystyrene plates (Pierce, Rockford, IL) were used to immobilize 50 μL of 1 mg/mL solution of SMA, and 50 μL of 4 peptides derived from the SMA sequence (residues 1-13, 43-52, 59-70, 94-107) (~1 mg/ml) and phosphate buffered saline control solution. After overnight incubation, the plate was blocked with 3% dried milk and 0.05 % Tween 80 in phosphate buffered saline. Then 0.01 mg/ml of the antibody 11-1F4 was added along with 3% dried milk, and 0.05% Tween 80 in phosphate buffered saline to each well. The plate was incubated overnight at 4°C. A solution of 0.05% Tween 80 in phosphate buffered saline was used to wash the plate in between incubations. A 100-fold dilution of fluorescent-labeled goat antimouse second antibody (Santa Cruz Biotechnology) was added to each well, again followed by washing the plate with 0.05% Tween 80 in phosphate-buffered saline. The fluorescence was then measured using a Cytofluor (Applied Biosystems) fluorescence plate reader.

Results and discussion

Structural and stability differences between LEN and SMA

The stability of LEN and SMA as a function of pH were determined using urea-induced denaturation (Table 1). Trp fluorescence was used to monitor the unfolding reaction. Typical data, for pH 6.0, are shown in Figure 2. The transitions were fit to a single unfolding transition and the apparent C_m determined: the term apparent is used since other data indicate that the starting conformation of SMA would not be the native conformation at acidic pH. Thus, conversion to free energy would be misleading, if interpreted as the change in ΔG from native to unfolded. The data clearly show that LEN is significantly more stable than SMA at all pH values (apparent ΔG values ≈ 1.5 kcal/mol). No significant change in Trp fluorescence was observed for SMA at pH 2, due to the fact that it is in a partially unfolded conformation in which the Trps are already solvent-exposed. Clearly, the increased stability of LEN must be a major factor in its resistance to fibrillation, compared to SMA.

Of the sequence differences between LEN and SMA, three residue differences (Y96Q, Q89H, and P40L) decrease the stability of LEN when incorporated individually, and only two, Q89H and T94H, involve ionizable side chains (Raffen *et al* 1999). Both the pH-dependence of Trp fluorescence and of ANS binding (see below, Figure 3) show significant differences between LEN and SMA, suggesting that part of the difference in their behavior reflects differences in one or more ionizable groups between them, most probably Q98H, although conformational changes induced by other residue differences could indirectly affect the pKs of other ionizable side chains.

Differences in population of partially-folded intermediates for LEN and SMA

Partially-folded intermediates are frequently populated under moderately destabilizing conditions, such as low pH or low concentrations of denaturant[26]. Several spectroscopic techniques, including intrinsic tryptophan fluorescence, 1,8-anilinonaphthalene sulfonate (ANS) binding, near- and far-UV circular dichroism, 1-D NMR and FTIR, were used to

Table 1. The effect of urea on the stability of LEN and SMA. The midpoints (C_m's) (M) of the unfolding transitions were calculated by curve fitting the change in intrinsic tryptophan fluorescence against urea concentration. The raw data was converted to fraction unfolded, no corrections for potentially different starting conformations were made. Standard errors were ±0.15 M.

pH	SMA	LEN
2.0	ND	1.92
4.0	1.47	3.22
6.0	3.24	5.26
8.0	4.02	5.22
10.0	3.49	4.39

ND: the conformation of SMA at pH 2 already has the Trp residues fully exposed and does not show significant changes in tryptophan fluorescence intensity upon addition of urea.

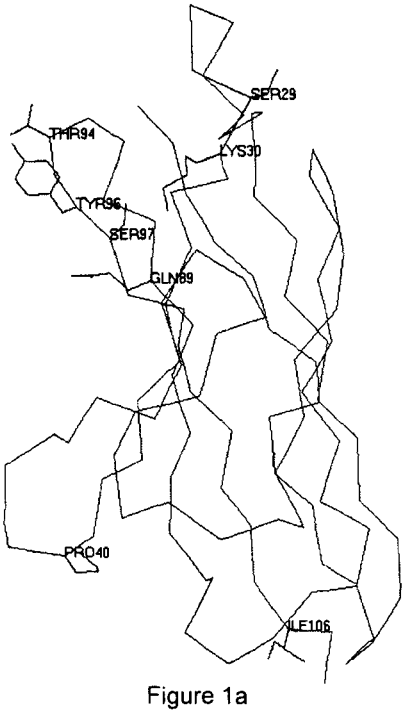

Figure 1a

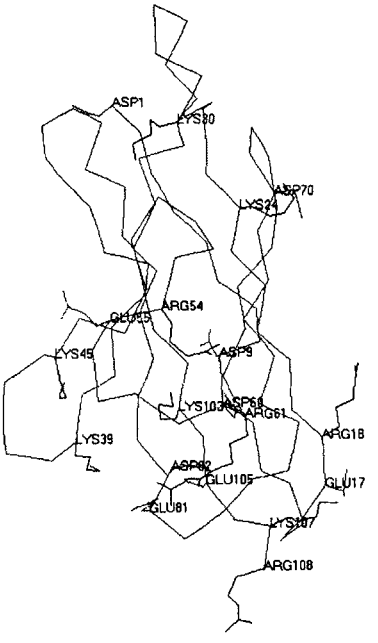

Figure 1b

FIGURE 1: Model of the crystal structure of LEN (PDB accession code 1LVE)[40], highlighting the amino acid residues that are different in SMA (left) and showing charged residues (lysines, arginines, aspartates and glutamates) (right). At low pH the salt bridges may be disrupted, and the histidines (positions 89,94) may repel each other and Lys-24, causing the protein to destabilize and ultimately form fibrils.

monitor tertiary and secondary structural changes as the pH of LEN and SMA was varied over the 8-2 range, in order to detect partially-folded intermediates. Two such intermediates were observed for SMA, a native-like one (I_N) populated between pH 4-5 and a relatively unfolded one (I_U) populated below pH 3; these have been described in detail previously[15]. No corresponding structural transitions were observed for LEN, as monitored by ANS binding, a common means of detecting partially-folded intermediates[27,28], in contrast to SMA, which showed two transitions in the ANS fluorescence emission maximum (Figure 3A) and changes in the ANS intensity[15]. The intensity of ANS emission below pH 3 was significantly higher than that of the native conformation of SMA (data not shown). The solid line fitted through the changes in ANS $_{max}$ versus pH for SMA (Figure 3A) was obtained using equation 2 (see **Materials and methods**), and yielded transition midpoints at pH 3.7±0.3 and 5.5±0.3.

The intrinsic tryptophan fluorescence emission was measured for LEN through the pH range 2-7.5 and compared with previously published data for SMA[15] by plotting either the wavelength of maximum emission (Figure 3B) or the emission intensity at 345 nm (Figure 3C). No significant changes were observed in either the wavelength of maximum emission or the emission intensity for LEN. The changes in the tryptophan emission maximum (Figure 3B) and intensity (Figure 3C) for SMA were fitted using equation 1 and the midpoints of the pH transition were 5.6±0.3 and 3.5±0.3 respectively. The λ_{max} for tryptophan fluorescence of SMA changed from 347 to 345 nm on lowering the pH to 5, indicative of changes in either one or both of the tryptophans to a more non-polar environment. No further change in the emission maxima was observed below pH 3. For SMA the intensity of tryptophan emission did not change significantly upon lowering the pH to 4, but a significant increase in the intensity was observed below pH 3. No significant change in tryptophan fluorescence intensity was observed for LEN, except for a small gradual increase with decreasing pH. The increase in fluorescence intensity for SMA on lowering the pH is attributed to a decrease in quenching of Trp 35 fluorescence caused by a conformational rearrangement in which Trp 35 is no longer in the vicinity of the disulfide bridge[15,18]. Such a conformational change was not observed for LEN. These observations confirmed that, in contrast to SMA, no significant tertiary structure changes occur for LEN on lowering the pH to 2.

Thus, no partially-folded intermediates equivalent to the I_N nor I_U intermediates of SMA were observed for LEN.

The apparent pK for the transition from native to I_N intermediate, with a pK of ~ 5.5 must directly or indirectly reflect the presence of a residue in SMA that is absent in LEN. If the former, it suggests the involvement of either one or both of the histidine residues that are present only in SMA. Two out of the eight residue differences between LEN and SMA are histidines (Q89H and T94H). These are the only residue differences that could involve an ionizable group in this pH range; however, the value is low for a histidine, suggesting that the imidazole sidechain is in a relatively non-polar environment to depress the pK. Alternatively, the pK could correspond to a carboxylate, whose environment is significantly difference in SMA relative to LEN. The available data do not allow an unambiguous choice between these two possibilities, although a His source is the simplest explanation. In either case, the residue changes in SMA result in a changes distinguishing the pH-dependence of SMA and LEN. Thus it is likely that the histidines may be important in the low pH conformational changes that are responsible for amyloid fibril formation selectively in SMA.

The transition from I_N to I_U in SMA, with a pK around 3.5, presumably involves one or more of the 4 aspartate or 2 glutamate residues (that do not change between LEN and SMA) whose environment changes significantly in SMA relative to LEN, to account for the observed titration. Histidines (Q89H and T94H) and glutamine (Y96Q) residue differences in SMA are also implicated in pH-dependent granular aggregate formation, which is not observed for LEN[5].

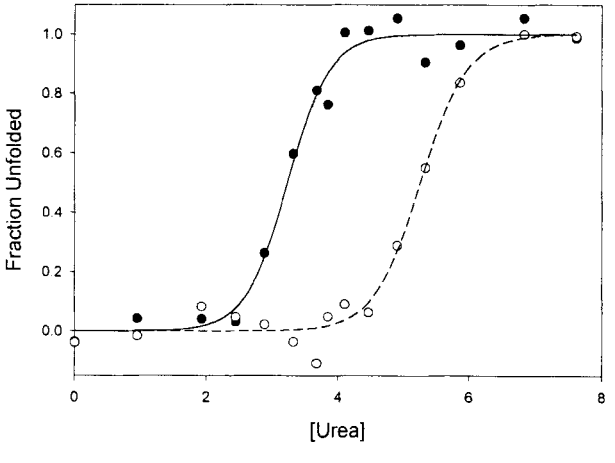

FIGURE 2: Urea-induced unfolding of SMA and LEN at pH 6.0, 37°C. The unfolding reaction was monitored by intrinsic Trp fluorescence and converted to fraction unfolded. The solid circles are for SMA, the open circles represent LEN.

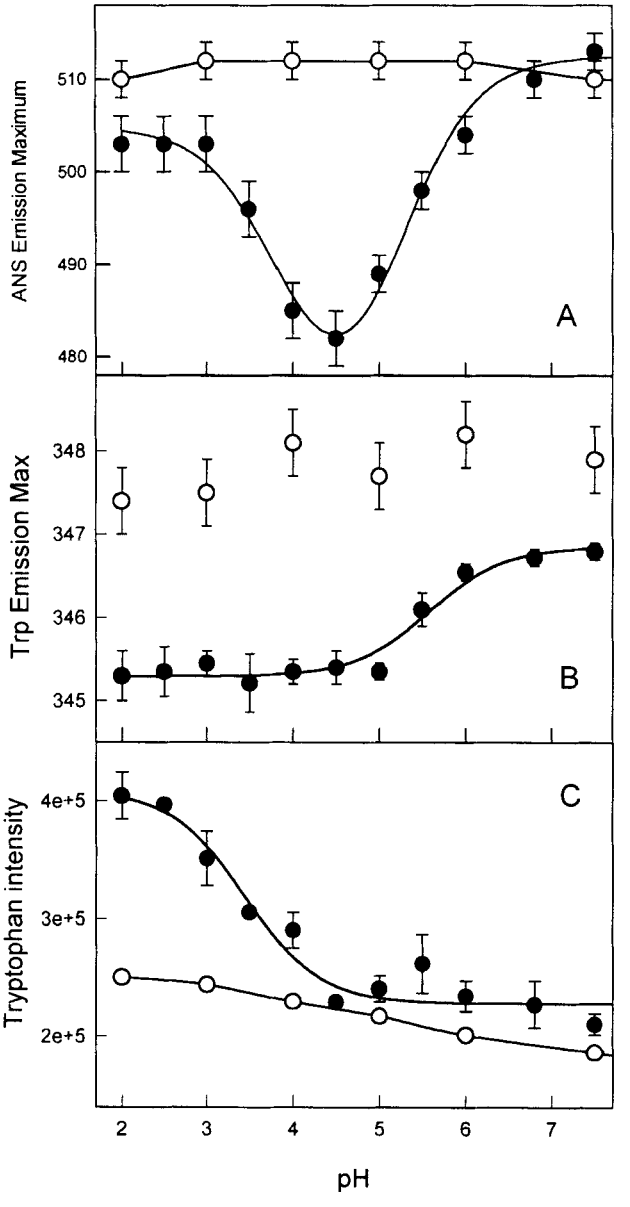

FIGURE 3: SMA, but not LEN, shows a build-up of partially folded intermediates on lowering the pH. Panel A: ANS binding in the pH range 2 to 7.5 for LEN (open symbols) and SMA (closed symbols), monitored by change in ANS fluorescence intensity. Panel B: The λ_{max} for tryptophan emission for SMA (closed symbols) and LEN (open symbols) over the pH range 2 to 7.5. Panel C: The tryptophan fluorescence intensity for SMA (closed symbols) and LEN (open symbols) over the pH range 2 to 7.5. The solid lines through SMA data are fitted to equation 1 and 2 as described in the materials and methods. No significant changes were observed for LEN upon lowering the pH whereas two transitions were apparent for SMA, leading to the formation of partially-folded intermediates I_N and I_U, respectively.

Secondary structure differences between LEN and SMA at low pH

We measured attenuated total reflectance FTIR spectra of SMA and LEN at both physiologic and acidic pH in order to compare their secondary structures. The amide I region (between 1600 and 1700 cm^{-1}) of the infrared spectrum is mainly contributed by the C=O bond stretching vibrations, and yields different peak positions for different types of secondary structure. Native LEN, native SMA and LEN at pH 2 all showed a major peak around 1638 cm^{-1} in the second derivative spectra of the amide I region, indicating predominantly β-structure (Figure 4). The similarity in the spectra of LEN at low pH to that of native LEN and native SMA indicates that the conformation of LEN has a very similar secondary structure at low pH as at neutral pH. In contrast, the conformation of SMA at pH below 3 was shown to have substantially altered secondary structure (Figure 4). A detailed comparison of curve-fitted spectra of native, I_N and I_U intermediates of SMA were described previously[15]. The data shown in Figure 4 confirmed LEN did not undergo significant structural reorganization at low pH, and that the conformation of LEN at pH 2 is native-like.

Circular dichroism spectra in both the far- and near-UV regions were recorded for SMA and LEN, to compare the low and high pH conformations. The low pH conformation of LEN closely resembled the neutral pH conformation of SMA (Figure 5). The far-UV CD spectra of LEN showed minor changes in the 216 nm peak upon lowering

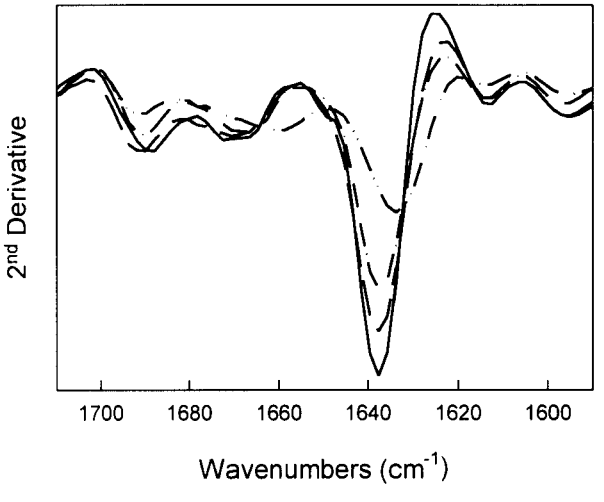

FIGURE 4: Differences in secondary structure between LEN and SMA monitored by FTIR. Second derivative ATR-FTIR spectra of the amide I region of SMA at pH 8 (——), LEN at pH 8 (— —), and SMA at pH 2 (— · · —) and LEN at pH 2 (— · —). The second derivative spectrum of SMA at pH 2 is different from the others, indicating a significant conformational change in the transition to the I_U intermediate conformation of SMA, whereas lowering the pH for LEN does not significantly alter its secondary structure

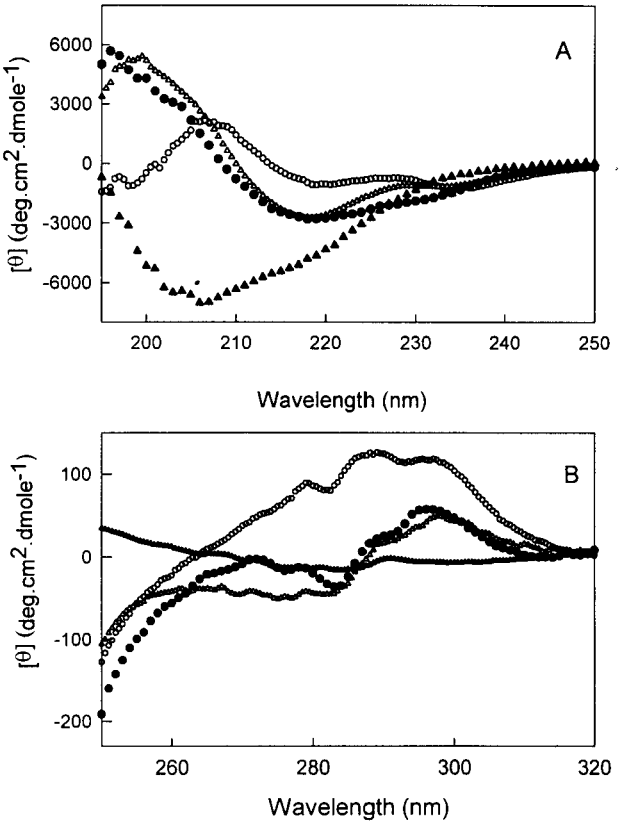

FIGURE 5: The low-pH conformation of LEN is similar to that of native SMA. Panel A: Far-UV CD, and Panel B: Near-UV CD spectra at pH 7.5 (circles) and pH 2.0 (triangles) for LEN (open symbols) and SMA (closed symbols). Both the far- and near-UV spectra of LEN at pH 2 are similar to those of native SMA. The I_U conformation (SMA at pH 2, the closed triangles) has significantly different spectra in both the far- and near-UV regions.

the pH from 8 to 2 (Figure 5A). Aromatic clusters are known to reduce the intensity of the ellipticity in the far-UV CD region, and sometimes to give rise to positive ellipticities at wavelengths as low as 216 nm[29]. In fact, the changes observed in the 216 nm peak in the spectrum of LEN on lowering the pH to 2 (Figure 5A) are probably due to changes in the aromatic clusters. This was confirmed by the lack of changes observed by infrared spectroscopy on lowering the pH (Figure 4). Notably, the far-UV CD spectrum of SMA at physiological pH was comparable to that of LEN at pH 2.

Significant changes in the near-UV spectrum of LEN on lowering the pH to 2 were observed, indicative of some changes in the aromatic clustering (Figure 5B). The near-UV CD spectrum of native SMA was comparable to that of LEN at pH 2 (Figure 5B). The CD data suggests that there may be some differences in the conformation of the aromatic clusters in native LEN compared to native SMA. However, the only aromatic residue change between LEN

and SMA (Y96Q) is not involved in either of the aromatic clusters. Lowering the pH of a LEN solution would neutralize the carboxylates, which could disrupt salt-bridges, causing changes in the orientation of the aromatic residues in LEN. Since both far- and near-UV CD spectra of LEN at low pH were similar to the native SMA spectrum, we suggest that the orientation of the aromatic clusters in the low pH conformation of LEN resembles that of native SMA. However, it should be noted that the changes in the near- and far-UV CD spectra of LEN at low pH do not seem to correlate with the behavior of the tryptophan, as seen in the data of Figure 3. Thus, the effects of decreased pH on the Trp environment do not parallel the changes in the aromatic clusters of LEN, in contrast to SMA.

It has been shown that proteins can be classified based on their conformation at low pH[30]. Based on this classification, LEN is identified as a type II protein, since it lost significant tertiary structure but maintained secondary upon lowering the pH. SMA on the other hand, underwent significant secondary and tertiary structure changes upon lowering the pH to 2.0 in the absence of salt, and is significantly unfolded. The addition of salt had no effect on the low pH conformation of SMA, and hence SMA is classified as a type I protein[30]. These differences are attributed to the lower stability of SMA.

Comparison of the kinetics of in vitro fibril formation of SMA and LEN

We chose to study fibril formation for LEN and SMA at pH 2, as these were the conditions that resulted in both most rapid kinetics and highest yield of fibrils. In the absence of agitation, only SMA formed fibrils at low pH (Figure 6A). LEN at low pH was monitored for 20 days at 37°C and no increase in thioflavin T was observed (data not shown). Figure 7 shows that changes in the Trp fluorescence of SMA, and ANS binding, correlated with the rate of fibrillation under conditions of no agitation, whereas no spectral changes were observed with LEN. The SMA spectral data also show an initial rapid change, attributed to formation of I_U.

With agitation, both proteins formed fibrils at low pH within a few hours. At low pH LEN began to form fibrils after 10 h (compared to 2 h for SMA) as shown by the increase in thioflavin T fluorescence (open symbols in Figure 6B). LEN also forms fibrils readily at 65°C, where the protein is partially denatured (data not shown), and in the presence of urea[17].

The 11-1F4 monoclonal antibody disassembles SMA fibrils and binds to one end of the protofilaments

We have previously shown, using atomic force microscopy (AFM), that the fibrillation of SMA involves a hierarchical assembly process[31] in which protofilaments (2.5 nm

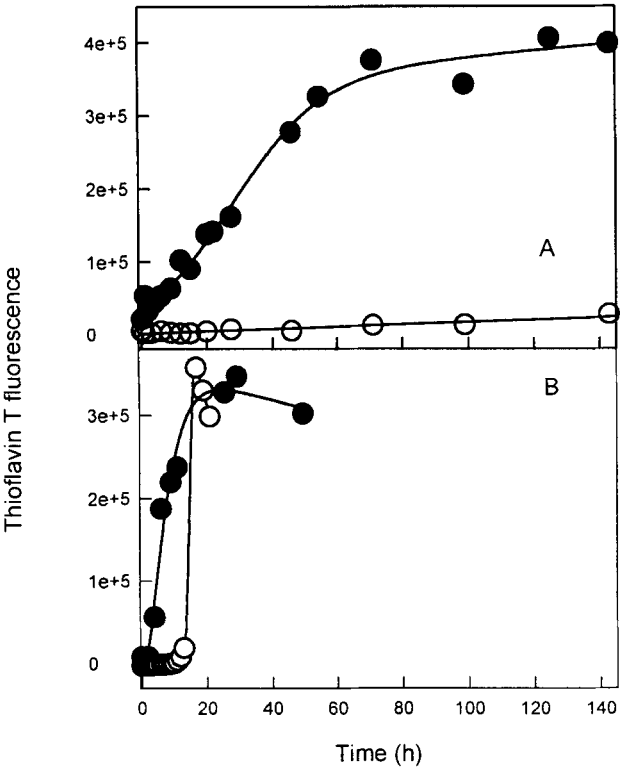

FIGURE 6: Comparison of the kinetics of fibril formation by SMA and LEN. Fibril formation was monitored by thioflavin T binding at pH 2, 37°C. Panel A: In the absence of agitation, LEN (open circles) and SMA (closed circles). No fibril formation was observed for LEN, whereas SMA formed fibrils readily. Panel B: In the presence of agitation (stirring at 600 rpm) both SMA and LEN formed fibrils, although the kinetics were faster for SMA. Protein concentration was 0.5 mg/ml.

diameter) are initially formed by elongation of fibril nuclei. Two of these protofilaments intertwine to form protofibrils (4.8 nm), and two protofibrils intertwine to form fibrils (8 nm). The 11-1F4 antibody was incubated with pre-formed SMA fibrils of 8 nm average diameter and fibril clusters formed at pH 5, where amorphous aggregates were also observed. The fibrils were separated from amorphous aggregates by spinning and separating the pellet fraction that populated amyloid fibrils. After 30 min incubation with the antibody only protofilaments of 2.5 nm diameter were observed by atomic force microscopy (white arrows in Figure 8). This observation means that the presence of the antibody led to rapid disassembly of fibrils into protofilaments.

This result strongly supports the hierarchical assembly model of fibril assembly. Further, the antibody-induced dissociation of the fibrils into protofilaments indicates that the antibody must interfere with the interaction of protofilaments to form protofibrils and fibrils. Interestingly, the 11-1F4 antibody was observed bound to only one end of the filaments, as shown by the light grey arrows in Figure 8. This

observation indicates that the monoclonal antibody specifically recognized one end of the filament and that the other end of the filament was thus structurally different; implying that the filament-forming subunit is asymmetric, and is joined end-to-end to form the filaments.

Amyloid fibrils formed at pH 2 for both LEN and SMA were also incubated with the 11-1F4 monoclonal antibody, and lead to dissolution of the fibrils, as no fibrils were observed by AFM after incubation with the antibody, indicating that the specific interaction of antibody to amyloid fibrils lead to their breakdown. In contrast, no binding of the kappa-specific monoclonal antibody 11-1F4 was observed on incubation with fibrils of insulin or alpha-synuclein, nor were these fibrils disrupted.

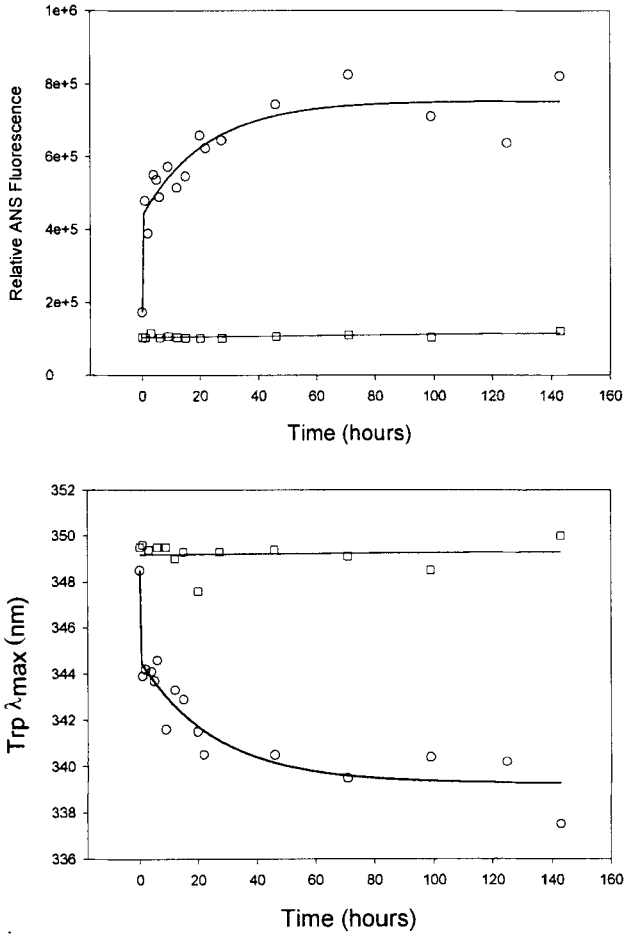

FIGURE 7: Spectral changes for LEN and SMA at pH 2.0, 37°C, no agitation. Open circles represent SMA, squares are for LEN. Top panel are changes in ANS fluorescence intensity, bottom panel is change in Trp fluorescence λ_{max}. The initial jump in the SMA data reflects formation of the I_U intermediate. Under these experimental conditions SMA formed fibrils with a similar rate to the slower observed spectral changes (see Figure 6A).

Elucidating the recognition site of 11-1F4

The solvent exposed β-strands of SMA, based on homology with the LEN crystal structure, were tested for recognition by the 11-1F4 antibody, using a fluorescence-conjugated secondary goat anti-mouse antibody and a plate assay. Of the four peptides tested, only the N-terminal peptide, DIVMTQSPDSLAV, was recognized by the 11-1F4 antibody (Figure 9). This result indicates that the 11-1F4 antibody specifically recognizes the N-terminal 13 residues of SMA. Thus, one end of the protofilament must have the N-terminal region of SMA exposed to solvent, so that it can be recognized by the monoclonal antibody.

Model for SMA fibrillation

The major differences in fibrillation properties between LEN and SMA must ultimately reflect their sequence differences. We would like to be able not only to propose a model for the mechanism of aggregation of SMA, but also to be able to account for its much greater propensity to fibrillate compared to LEN. One significant difference between LEN and SMA is that in the latter, long-lived partially-folded intermediates are present, which are absent in LEN. Since we believe that such partially-folded intermediates are critical precursors for aggregation, the larger their population the greater the propensity to fibrillate. In the case of LEN, our data indicate that if there are corresponding partially-folded intermediates to those of SMA, they are populated to much lower levels or are much more short-lived. The lack of such stabilized intermediate conformations for LEN is the most likely reason for its greatly decreased propensity to fibrillate, in comparison with SMA. This then leads to the question of why SMA forms such intermediates and LEN does not. We have previously reported that the relatively native-like partially folded intermediate of SMA (I_N) is responsible for amorphous aggregates, and the more unfolded partially-folded intermediate (I_U) is critical for fibril formation[15]. Since only fibrils are formed by LEN on agitation at low pH[16] it is likely that under these conditions LEN forms transient intermediates with similar properties to I_U. Apparently the significantly greater stability of LEN, due to the Y96Q, Q89H, and P40L substitutions, decreases the population of the LEN partially-folded intermediate(s) to the point where low pH alone is insufficiently destabilizing to populate the intermediate to a high enough concentration to form the critical nucleus leading to fibrillation. It is only with the additional destabilizing influence of the air-water interface (on agitation) or the presence of denaturants such as urea[17] that sufficient partially-folded intermediate(s) of LEN build-up to allow fibrillation to occur.

The kinetics of SMA fibrillation are consistent with a scheme involving nucleated polymerization, which is characterized by a lag followed by exponential growth of fibrils. Given the critical requirement for the I_U intermediate for

fibrillation, the minimum kinetic scheme for SMA fibrillation is shown in scheme 1,

$$M \Leftrightarrow I_U \Leftrightarrow \text{Nucleus} \rightarrow \text{Fibrils}$$

Scheme 1

where M = native monomer and I_U = relatively unfolded intermediate. In the case of LEN we assume a similar scheme exists, except that the partially-folded intermediates are only transiently populated, and only under conditions of significant destabilization, e.g. low pH and agitation. However, the presence of amorphous aggregates with SMA[15], and off-pathway oligomers with LEN[16] indicates that the actual overall aggregation pathways are considerably more complex, minimally as shown in scheme 2,

$$M \Leftrightarrow (I) \Leftrightarrow \text{Nucleus} \rightarrow \text{Fibrils}$$

$$(I)_n \longrightarrow \text{Amorphous aggregates}$$

Scheme 2

where (I) represents one or more partially folded intermediate and $(I)_n$ represents oligomeric intermediate(s).

The AFM results, demonstrating that an antibody that recognizes the N-terminal residues of SMA can disassemble SMA fibrils into protofilaments, and that the antibody preferentially binds to one end of the protofilaments, are informative. The latter observation indicates that the protofilaments have directionality (see Figure 8), and that the N-terminal strand is only accessible to the antibody at one end of the protofilament. Since the protofilaments are 2.5 nm high, they may either represent a single molecule of SMA in cross-section, i. e. the β-strands with their attendant turns and loops run orthogonal to the axis of the filament and the mica substrate, or they may represent two SMA molecules in cross-section, one β-sheet stacked on top of another. Based on the far-UV circular dichroism and FTIR spectra of the I_U intermediate it is possible this intermediate still retains a significant native-like topology for its β-strands. The AFM data are consistent with a model in which the N-terminal strand of one I_U molecule can interact with the C-terminal strand of another, leading to indefinite elongation (Figure 10). Interestingly, the injection of light chain antibodies into mouse amyloidomas has been reported to result in antibody-induced regression[32]. That the presence of the antibody binding to one end of the protofilaments is sufficient to rapidly dissociate fibrils and protofibrils into their constituent protofilaments suggests that the forces involved in the interaction between the protofilaments are relatively weak. The simplest explanation would involve binding of the antibody at one end of the protofilament acting as a wedge to physically separate the protofilament components of the fibrils and protofibrils.

Although there have been few detailed structural characterizations of partially-folded intermediates, the data that are available suggest that they consist of a core of native-like structure with the remainder of the polypeptide chain in a highly dynamic state, but favoring native-like conformations[33-36]. Thus for molecules such as the light chain variable domains, the partially-folded intermediates are likely to consist of a core of β-strands with the N- and C-terminal

FIGURE 8: Atomic force microscopy images of SMA fibrils interacting with a κIV-specific monoclonal antibody, 11-1F4. This antibody, which recognizes the N-terminal residues of SMA, binds only to one end of SMA protofilaments, and causes "unwinding" of SMA fibrils to their constituent protofilaments. Panel A: antibody molecules (light grey arrows) bound to the ends of SMA protofilaments (white arrows; 2.5 nm in diameter; the starting fibrils were 8 nm high). Panel B: one 11-1F4 molecule binding to two filaments (arrow), indicating that both the antigen binding sites of the monoclonal antibody bound one end of two different filaments.

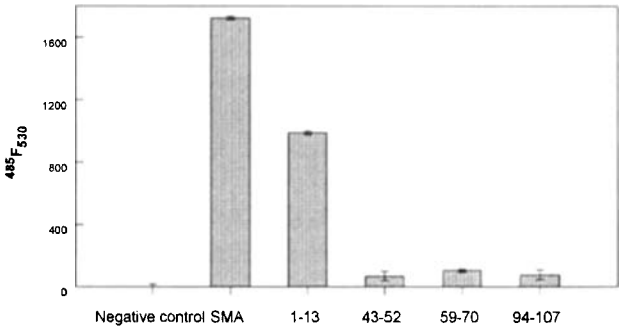

FIGURE 9: Elucidation of the 11-1F4 monoclonal antibody recognition site on the κIV variable domain sequence. The binding of the following potential antigens; buffer (negative control), purified SMA, four peptides derived from the SMA sequence, residues 1-13, 43-52, 59-70 and 94-107, was done as described in the experimental procedures. The fluorescence values from binding of a fluorescence-labeled secondary antibody are shown as the ordinate.

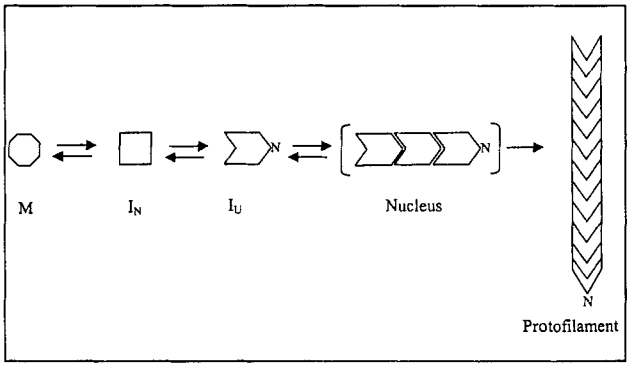

FIGURE 10: Minimal kinetic scheme for the fibrillation pathway for SMA. The model shows the conformational change between native monomer (M) to two partially-folded intermediates (I_N which leads predominantly to amorphous aggregates, and I_U which leads to fibrils) of which I_U is asymmetric and assembles in the nucleus and fibrils with distinct N- and C-terminal polarity, as shown by the letter N. Protofilaments, which are shown, interact to form protofibrils and fibrils.

regions relatively unfolded. In addition, the core structure of SMA and LEN will be maintained by the single disulfide bridge formed between Cys23 and Cys88.

Thus, it is possible that the intermolecular interactions between individual molecules of SMA in the formation of protofilaments involve an interaction that may be likened to a domain swap between the N-terminal strand of one molecule with the C-terminal strand of another. This is analogous to the models proposed for the dimerization of RNase A. For RNase A, major[37] and minor dimers[38] are formed by domain swapping of either the C- or the N-terminal parts, respectively. Further interactions between the N-terminal of one molecule and the C-terminal of another molecule can result in the infinite formation of long fibril-like structures. The monoclonal antibody binding to one end of SMA protofilaments directly implicates the involvement of the N-terminal end of the molecule. Since the N- and C-terminal regions directly interact in the native conformation, we propose that the C-terminal end is the other most likely region that could be involved in asymmetric domain swapping resulting in long amyloid fibrils.

Davis *et al*[5,39] suggest that peptides FTLTISS (71-77) and YQQKPGQ (36-42) function as inhibitors of fibril formation and granular aggregate formation in SMA respectively. It is possible that that these residues are directly involved in intermolecular interactions and hence block the regions of the protein that are involved in elongation of amyloid fibrils or granular aggregate formation, as the case may be.

Two of the amino acid differences between LEN and SMA, Q89H and T94H, lead to differences in charge at low pH between the two proteins. The two histidines, present only in SMA will be positively charged at low pH (below 5), and could lead to additional charge-charge repulsion, both with each other and also with Lys24, the only other positively charged residue in their vicinity. This repulsion could cause the loop prior to the C-terminal β-strand to pull away from the core structure. Lowering the pH could also disrupt the salt-bridges between Asp9-Lys103 (connecting the N- and C-terminal strands) and Lys107-Glu17 in both LEN and SMA (Figure 1). LEN, on the other hand, does not undergo conformational changes upon lowering the pH, possibly due to the absence of the two histidine residues at positions 89 and 94. This could indicate that it is the easier swapping of the C-terminal strand of SMA, due to weaker interactions with the core of the molecule, which facilitates fibrillation.

The data allow us to correlate the differences in primary structure of a benign and an amyloidogenic light chain directly to their fibril-forming propensities. These observations broaden the hypothesis that the primary structure encodes the information for the native conformation. We propose that the primary structure may also determine conformational changes leading to aggregation.

Acknowledgments

This research was supported by grants from the NIH (DK55675) (ALF) and NSF (CHE-9987824).

References

1 Cohen, AS and Jones, LA (1991). Amyloidosis. *Curr Opin Rheumatol* **3**, 125-138

2 Sipe, JD (1994). Amyloidosis. *Crit Rev Clin Lab Sci* **31**, 325-54

3 Buxbaum, JN, Chuba, JV, Hellman, GC, Solomon, A and Gallo, GR (1990). Monoclonal immunoglobulin deposition disease: light chain and light and heavy chain deposition diseases and their relation to light chain amyloidosis. Clinical features, immunopathology, and molecular analysis. *Ann Intern Med* **112**, 455-64

4 Stevens, FJ, Solomon, A and Schiffer, M (1991). Bence Jones proteins: a powerful tool for the fundamental study of protein chemistry and pathophysiology. *Biochemistry* **30**, 6803-5

5 Davis, DP, Gallo, G, Vogen, SM, Dul, JL, Sciarretta, KL, Kumar, A, Raffen, R, Stevens, FJ and Argon, Y (2001). Both the environment and somatic mutations govern the aggregation pathway of pathogenic immunoglobulin light chain. *J Mol Biol* **313**, 1021-1034

6 Bellotti, V and Merlini, G (1996). Current concepts on the pathogenesis of systemic amyloidosis. *Nephrol Dial Transplant* **11 Suppl 9**, 53-62

7 Hurle, MR, Helms, LR, Li, L, Chan, W and Wetzel, R (1994). A role for destabilizing amino acid replacements in light-chain amyloidosis. *Proc Natl Acad Sci U S A* **91**, 5446-50

8 Stevens, FJ, Myatt, EA, Chang, CH, Westholm, FA, Eulitz, M, Weiss, DT, Murphy, C, Solomon, A and Schiffer, M (1995). A molecular model for self-assembly of amyloid fibrils: immunoglobulin light chains. *Biochemistry* **34**, 10697-702

9 Kim, Y, Wall, JS, Meyer, J, Murphy, C, Randolph, TW, Manning, MC, Solomon, A and Carpenter, JF (2000). Thermodynamic modulation of light chain amyloid fibril formation. *J Biol Chem* **275**, 1570-1574

10 Merlini, G, Bellotti, V, Andreola, A, Palladini, G, Obici, L, Casarini, S and Perfetti, V (2001). Protein aggregation. *Clin Chem Lab Med* **39**, 1065-1075

11 Pras, M, Schubert, M, Zucker-Franklin, D, Rimon, A and Franklin, EC (1968). The characterization of soluble amyloid prepared in water. *J Clin Invest* **47**, 924-33

12 Solomon, A (1985). Light chains of human immunoglobulins. *Methods Enzymol* 116:101-21

13 Raffen, R, Dieckman, LJ, Szpunar, M, Wunschl, C, Pokkuluri, PR, Dave, P, Wilkins, SP, Cai, X, Schiffer, M and Stevens, FJ (1999). Physicochemical consequences of amino acid variations that contribute to fibril formation by immunoglobulin light chains. *Protein Sci* **8**, 509-517

14 Huang, DB, Chang, CH, Ainsworth, C, Johnson, G, Solomon, A, Stevens, FJ and Schiffer, M (1997). Variable domain structure of kappaIV human light chain Len: high homology to the murine light chain McPC603. *Mol. Immunol* **34**, 1291-1301

15 Khurana, R, Gillespie, JR, Talapatra, A, Minert, LJ, Ionescu-Zanetti, C, Millett, I and Fink, AL (2001). Partially folded intermediates as critical precursors of light chain amyloid fibrils and amorphous aggregates. *Biochemistry* **40**, 3525-3535

16 Souillac, PO, Uversky, VN, Millett, IS, Khurana, R, Doniach, S and Fink, AL (2002). Elucidation of the molecular mechanism during the early events in immunoglobulin light chain amyloid fibrillation: Evidence for an off-pathway oligomer at acidic pH. *J. Biol Chem* **277**, 12657-12665

17 Souillac, PO, Uversky, VN, Millett, IS, Khurana, R, Doniach, S and Fink, AL (2002). Effect of association state and conformational stability on the kinetics of immunoglobulin light chain amyloid fibril formation at physiological pH. *J Biol Chem* **277**, 12657-12665

18 Stevens, PW, Raffen, R, Hanson, DK, Deng, YL, Berrios-Hammond, M, Westholm, FA, Murphy, C, Eulitz, M, Wetzel, R, Solomon, A, Schiffer, M and Stevens, FJ (1995). Recombinant immunoglobulin variable domains generated from synthetic genes provide a system for in vitro characterization of light-chain amyloid proteins. *Protein Sci* **4**, 421-432

19 Khurana, R, Hate, AT, Nath, U and Udgaonkar, JB (1995). pH dependence of the stability of barstar to chemical and thermal denaturation. *Protein Sci* **4**, 1133-1144

20 Oberg, K. A. & Fink, A. L. (1995). Methods for Collecting and Analyzing Attenuated Total Reflectance FTIR Spectra of Proteins in Solution. In *Techniques in Protein Chemistry* (W.Crabb, ed), pp. 475-484, Academic Press, Inc.

21 Oberg, KA and Fink, AL (1998). A new attenuated total reflectance Fourier transform infrared spectroscopy method for the study of proteins in solution. *Anal Biochem* **256**, 92-106

22 Seshadri, S, Khurana, R and Fink, AL (1999). FTIR Analysis of Protein Deposits. *Methods in Enzymology* **309**, 559-576

23 Naiki, H, Higuchi, K, Hosokawa, M and Takeda, T (1989). Fluorometric determination of amyloid fibrils in vitro using the fluorescent dye, thioflavin T1. *Anal Biochem* **177**, 244-249

24 Levine, H (1993). Thioflavine-T Interaction with Synthetic Alzheimers Disease ß-Amyloid Peptides - Detection of Amyloid Aggregation in Solution. *Protein Science* **2**, 404-410

25 Abe, M, Goto, T, Wolfenbarger, D, Weiss, DT and Solomon, A (1993). Novel immunization protocol and ELISA screening methods used to obtain and characterize monoclonal antibodies specific for human light chain variable-region subgroups. *Hybridoma* **12**, 475-483

26 Fink, AL (1995). Compact intermediate states in protein folding. *Annu Rev Biophys Biomol Struct* **24**, 495-522

27 Semisotnov, GV, Rodionova, NA, Razgulyaev, OI, Uversky, VN, Gripas', AF and Gilmanshin, RI (1991). Study of the "molten globule" intermediate state in protein folding by a hydrophobic fluorescent probe. *Biopolymers* **31**, 119-28

28 Goto, Y and Fink, AL (1989). Conformational states of beta-lactamase: molten-globule states at acidic and alkaline pH with high salt. *Biochemistry* **28**, 945-52

29 Zaremba, SM and Gregoret, LM (1999). Context-dependence of amino acid residue pairing in antiparallel beta-sheets. *J Mol Biol* **291**, 463-479

30 Fink, AL, Calciano, LJ, Goto, Y, Kurotsu, T and Palleros, DR (1994). Classification of acid denaturation of proteins - intermediates and unfolded states. *Biochemistry* **33**, 12504-12511

31 Ionescu-Zanetti, C, Khurana, R, Gillespie, JR, Petrick, JS, Trabachino, LC, Minert, LJ, Carter, SA and Fink, AL (1999).

Monitoring the assembly of Ig light-chain amyloid fibrils by atomic force microscopy. *Proc Natl Acad Sci USA* **96**, 13175-13179

32 Hrncic, R, Wall, J, Wolfenbarger, DA, Murphy, CL, Schell, M, Weiss, DT and Solomon, A (2000). Antibody-mediated resolution of light chain-associated amyloid deposits. *Am J Pathol* **157**, 1239-1246

33 Gillespie, JR and Shortle, D (1997). Characterization of Long-Range Structure in the Denatured State of Staphylococcal Nuclease .1. Paramagnetic Relaxation Enhancement by Nitroxide Spin Labels. *J Mol Biol* **268**, 158-169

34 Wang and Shortle (1997). Residual helical and turn structure in the denatured state of staphylococcal nuclease: analysis of peptide fragments. *Folding & Design* **2**, 93-100

35 Yao, J, Chung, J, Eliezer, D, Wright, PE and Dyson, HJ (2001). NMR structural and dynamic characterization of the acid-unfolded state of apomyoglobin provides insights into the early events in protein folding. *Biochemistry* **40**, 3561-3571

36 Eliezer, D, Chung, J, Dyson, HJ and Wright, PE (2000). Native and non-native secondary structure and dynamics in the pH 4 intermediate of apomyoglobin. *Biochemistry* **39**, 2894-2901

37 Liu, Y, Gotte, G, Libonati, M and Eisenberg, D (2001). A domain-swapped RNase A dimer with implications for amyloid formation. *Nat Struct Biol* **8**, 211-214

38 Liu, Y, Hart, PJ, Schlunegger, MP and Eisenberg, D (1998). The crystal structure of a 3D domain-swapped dimer of RNase A at a 2.1-A resolution. *Proc Natl Acad Sci USA* **95**, 3437-3442

39 Davis, PD, Raffen, R, Dul, LJ, Vogen, MS, Williamson, KE, Stevens, JF and Argon, Y (2000). Inhibition of amyloid fiber assembly by both BiP and its target peptide. *Immunity* **13**, 433-442

40 Huang, DB, Chang, CH, Ainsworth, C, Johnson, G, Solomon, A, Stevens, FJ and Schiffer, M (1997). Variable domain structure of kappaIV human light chain Len: high. *Mol Immunol* **34**, 1291-301